Ethiopian Journal of Water Science and Technology (EJWST)

DOI: https://doi.org/10.59122/EJWST658

Vol. 9, 2026, Pages: 1~31 ISSN (Print): 2220-7643

Modeling Future Climate Change Impacts on Precipitation Pattern Using a Multi-Model Ensemble of CMIP6 Scenarios for the Abaya-Chamo Sub-Basin, Ethiopia

Desalegn Laelago Ersado [1, 2, *], Admasu Gebeyehu Awoke[1]

[1]School of Civil and Environmental Engineering, Addis Ababa Institute of Technology(AAiT), Addis Ababa University, Post Office Box: 1176, Addis Ababa, Ethiopia
[2]Department of Hydraulics and Water Resources Engineering, Hawassa Institute of Technology, Hawassa University, Post Office Box: 05, Hawassa, Ethiopia

***Corresponding author:** Desalegn Laelago Ersado: desalegnlog@gmail.com/, https://orcid.org/0000-0001-9556-1908

Abstract

Climate change disrupts the natural water cycle and agriculture, hindering the progress toward achieving sustainable development goals. Employing bias-corrected climate model simulations is crucial for future climate change patterns prediction and informing policy decisions. This research employs a multi-model ensemble from the Coupled Model Intercomparison Project Phase 6 to assess how climate change affects precipitation patterns in the Abaya-Chamo Sub-basin located in southern Ethiopia. Future predicted precipitation datasets were evaluated under Shared Socioeconomic Pathway scenarios. The Climate Data Operators (CDOs) tool was used to interpolate global climate model results. A power transformation method was utilized to address systematic biases in the outputs of the multi-model ensemble. Spatial patterns of precipitation maps in ArcMap were generated using the inverse distance weighting method. The findings revealed that the bias-corrected mean monthly and annual precipitations were lower than the observed precipitations. The SSP2-4.5 scenario forecasted a decrease in mean annual precipitation of 6.6% to 25.85% over the near periods (2021-2064) and a decrease of 2.25% to 20.24% in the long term future (2065-2100). The spring (MAM) season experienced the largest percentage reduction of all seasons. The spatial distribution of mean annual precipitation varied widely across watersheds, ranging from 450 to 1,140 millimeters. The multi-model ensemble projection for precipitation indicates a more significant decrease in the Gidabo watersheds during the summer (JJA) and spring (MAM) seasons, highlighting spatial variability. Projected future precipitation declines are expected to reduce the amount of water available to ecosystems. Therefore, developing comprehensive, effective water resource management strategies is extremely important to adapt to these changes.

Keywords: Abaya-Chamo, Bias Correction, CMIP6, Climate Change, Multi-Model Ensemble, Precipitation.

Received: 25 Novmeber, 2025; Accepted: 01 January, 2026 Published: 27 February 2026

1 INTRODUCTION

Global climate variation is a critical challenge of the world in the twenty-first century. This can be expressed in terms of increasing mean temperature (Suksatit et al., 2025). Furthermore, climate change causes a rise of at least 2°C in worldwide surface temperatures, which in turn causes difficulties in achieving sustainable development goals (IPCC, 2022). Climate change significantly changes the amount of water stored on Earth and impacts hydrological extremes like droughts and floods (Gurara et al., 2021). Moreover, climate variability modifies the natural hydrological cycle that connects groundwater, surface water, and precipitation (Umugwaneza et al., 2021). The natural changes potentially lead to serious water scarcity (Umugwaneza et al., 2021).

The effects of climate change are particularly high in developing countries because they have limited adaptive capacity (Omay et al., 2023). For instance, a study by Ayugi et al. (2022) in East Africa showed that the local population was affected by the diverse impacts of climate change, including severe precipitation fluctuations across different levels of global warming. Although rising temperatures and changes in precipitation patterns were observed in Africa in the 21st century (Almazroui et al., 2020). Similarly, climate change presents considerable challenge to Ethiopia; particularly it affects its agricultural economy and the management of hydrological resources (Belay et al., 2021; Rettie et al., 2023). For instance, Ayalew (2023) employed high-resolution climate model projection outputs to analyze the spatial-temporal inconsistencies of climate and its impact on rainfall distribution within the Hare Catchment.His findings indicated a significant reduction in precipitation distribution (Ayalew, 2023).However, in the upper Blue Nile Basin, increasing variability was observed in annual precipitation and temperature (Enawgaw et al., 2023). Therefore, assessing the potential impact of climate change on hydrological systems at different watershed scales is important to characterize the heterogeneous nature of precipitation changes in Ethiopia. Moreover, the climate change impact assessment helped to develop adaptation techniques in water management system (Umugwaneza et al., 2021).

The effect of climate change and future climate change trends prediction can be estimated using climate models (IPCC, 2022). General circulation models are applied to evaluate the impact of climate variation on future hydrological response scenarios and water supply sources (Alotaibi et

al., 2018; Chang et al., 2018). Furthermore, GCM models are used to predict meteorological parameters under various future climatic conditions (Almazroui et al., 2021). However, global climate model projections are influenced by various uncertainties. Uncertainties of climate change projections stem from model selection formulation, differing emission scenarios, internal climate variability, and regional discrepancies (Almazroui et al., 2020; Deser et al., 2012). The presence of these uncertainties can significantly impact the reliability of climate predictions for adaptation planning (Deser et al., 2012). Therefore, the identification of common sources of uncertainties is important during the analysis of climate change.

General Circulation Models (GCMs) simulate climatic parameters at the level of a grid cell or coarse resolution scale (Rettie et al., 2023). Downscaling converts coarse-resolution GCM output into local-scale detail needed for further application of GCM output and hydrological simulation (Rettie et al., 2023). Due to the significant biases present in GCMs and the high level of uncertainty, relying solely on downscaled climate model projections is generally insufficient for direct use in regional climate change impact studies (Onyutha et al., 2021). The accuracy of a climate change projection is enhanced by using multi-model ensemble approaches: the statistical downscaling to localized contexts, and bias correction of model results (Rettie et al., 2023). In this regard, Jamal et al.(2023) applied the ensemble mean of seven model outputs to test observed past climate patterns and future climate projections. The result indicated that the mean-based bias-corrected multi-model ensemble (MME) performed well compared to individual models, replicating the reference datasets (Jamal et al., 2023). Mean-based bias correction techniques provided long-term precipitation and temperature projection by accounting a nonlinear ensemble dynamics of GCMs (Jamal et al., 2023). Similarly, Wen et al.(2021) analyzed the impact of future climate change on runoff using four CMIP6 downscaled and bias-corrected ensemble models dataset in the Amur River Basin.

Climate model bias refers to the deviation between observed measurements and the outputs generated by climate models (Gurara et al., 2021). Many researchers have implemented various bias correction techniques for coarse-resolution GCM data output (Rastogi et al., 2022; Voudouris, 2022). For instance, Rettie et al. (2023) applied bias correction techniques to produce 10 km spatial resolution climate change projections from coarse-resolution climate model outputs. However, a few studies analyzed the impact of climate change on precipitation

distribution in the Abaya-Chamo Sub-basin (Ayalew, 2023; Demmissie et al., 2018; Temesgen et al., 2022). For example, Ayalew (2023) utilized seven regional climate models (RCMs) to examine the spatio-temporal patterns of climate change effects on the distribution of hydro-meteorological variables in the Hare Catchment.

This study primarily aimed to examine how global climate change affected historical and future precipitation patterns under medium (SSP2-4.5) and high (SSP5-8.5) emission scenarios in the Abaya-Chamo Sub-basin. The selected best-performing CMIP6 multi-model ensemble results were downscaled to the local scale and bias corrected. The selected GCMs' outputs were extracted and interpolated using the climate data operators' tool. The Power Transformation (PT) method was employed to adjust and correct the multi-model ensemble GCM outputs' biases. Thus, this study offers critical insights into projected future precipitation patterns and informs strategies for climate-resilient development. Furthermore, it offers valuable insight for policymakers into anticipated future rainfall trends and aids in shaping strategies for climate-resilient development.

2 MATERIALS AND METHODS

2.1 Description of the Study Area

This research was conducted in the Abaya-Chamo Sub-basin of the Rift Valley Lakes Basin in southern Ethiopia. The Ethiopian Rift Valley Lakes Basin is characterized by perennial rivers and an interconnected network of lakes formed through geological processes related to the East African Rift System (Ayenew & Legesse, 2007). The region is located 5°52'N to 8°8'N latitude, and 37°16'E to 38°39.5'E longitude (Figure 1). The study area is characterized by transitive changes in landforms, physical features, and climatic conditions (Molla et al., 2019). The sub-basins drain into Lakes Abaya and Chamo, formed by volcanic activity (Gebeyehu, Chunju, Yihong, et al., 2019). The sub-basin also includes Nech Sar National Park in addition to the interconnected rivers (Hussen & Wagesho, 2016). Gelana, Bilate, Gidabo, Hare, Baso, and Hamessa-Amessa rivers are the main rivers that drain into Abaya Lake. The Sile, Argoba, Wezeka, Sego, Abaya as well as the Kulfo River drain into Chamo Lake (Hussen & Wagesho, 2016).

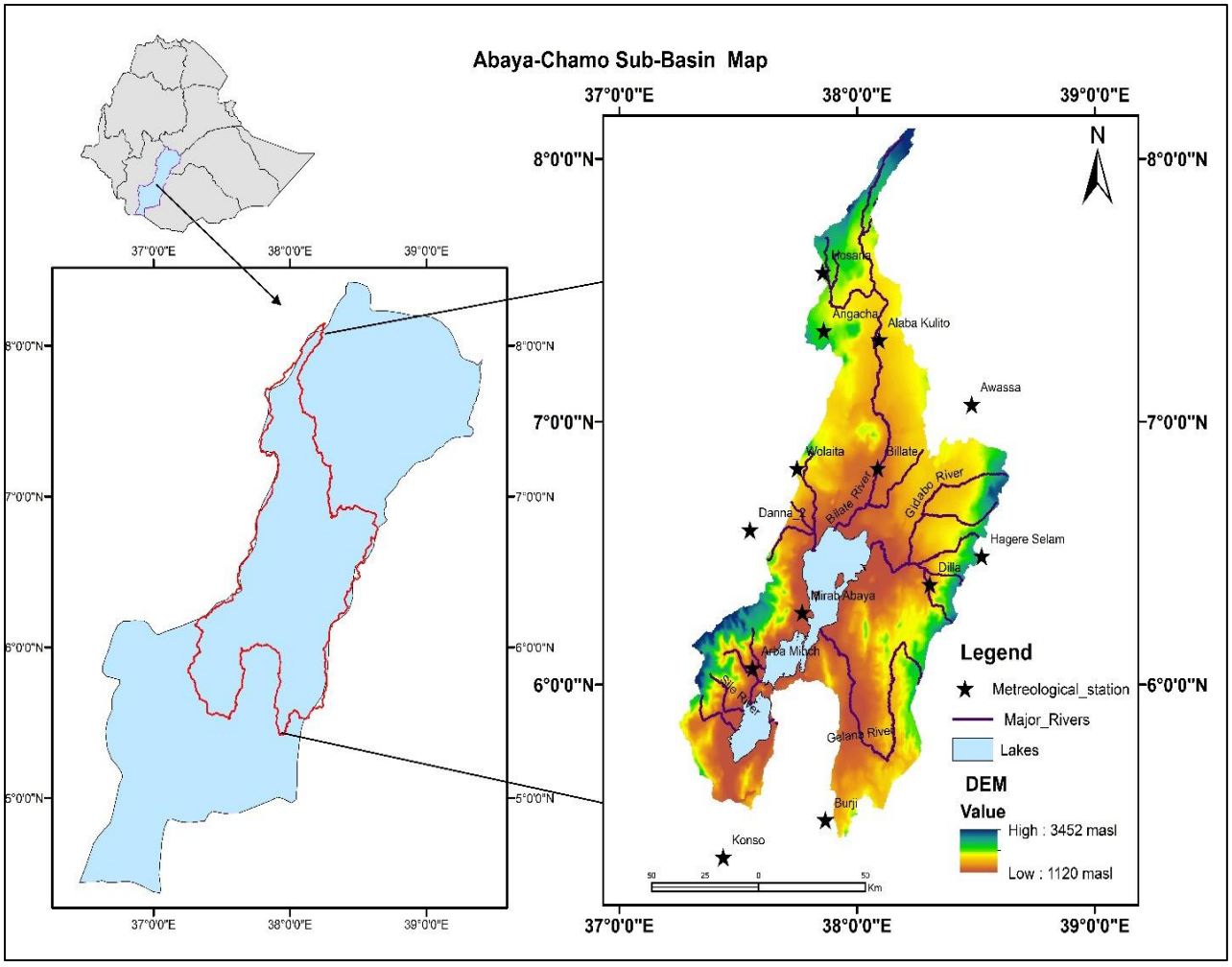

Figure 1 | Abaya-Chamo Sub-basin location map, selected meteorological stations, digital elevation model (DEM) with meters above sea level (masl) to indicate elevation

The total drainage-basin area of the Abaya-Chamo Sub-basin, including freshwater bodies, is 18,600 km². Its altitudes range from 1,120 m to 3,452 m above mean sea level (masl) (Figure 1). The mean annual precipitation ranges from approximately 400 mm to 2,300 mm (Gebeyehu, Chunju, Yihong, et al., 2019).

2.1 Data sets

2.1.1 Observed Meteorological Datasets

The daily precipitation observations were acquired from the National Meteorological Agency. Thirteen recording stations within and near the study area were considered (Figure 1) for analysis. The location of the station, data availability range, and data quality were considered for further analysis of meteorological stations (Stawowy et al., 2021). According to the World Meteorological Organization, the decision to include or exclude a station for analysis is based on

the number of years (WMO, 2011). The eleven stations located in Arba Minchincluded: Danna_2, Konso, Mirab_Abaya, Alaba Kulito, Angacha, Hosana, Awassa, Billate-Tena, Dilla, and Wolaita. These stations were selected for their strong location representation and good data from 1992–2020. The collected raw data were processed to fill the missing data and check for consistency.

The missing precipitation and temperature data were usually estimated using the arithmetic mean, normal ratio, or inverse distance weighting methods (Boke, 2017; Hırca & Eryılmaz Türkkan, 2024; Mahyun et al., 2024). In this study, the Inverse Distance Weighted (IDW) interpolation technique was selected to estimate the missing precipitation values. This method was selected because of its simplicity and effectiveness in estimating missing meteorological data (Al-husban, 2022; Belay et al., 2021; Chin et al., 2023). According to the Inverse Distance Weighted method, weather stations located closer to a target point had more influence and carried more weight in determining the interpolated value than stations situated farther away (Chin et al., 2023). The IDW is calculated using the following formula (Equation 1):

$$P_x = \frac{\sum_{i=1}^{i=n} \frac{1}{d^q} P_i}{\sum_{i=1}^{i=n} \frac{1}{d^q}} \quad (1)$$

Where Px is the filled precipitation at the target station, P_i is the observed value at the i^{th} nearby station, d is the distance between them, q is commonly set to 2, and n is the total number of neighboring selected stations. Most of the observed precipitation data stations in the region were found to have missing values ranging from 0.03% to 13.37%. The selected observed data stations had less than 10% missing data and more than twenty-eight years of records. Table 1 shows the geographic locations and data recording details of the eleven meteorological stations.

Daily datasets with complete and non-missing climate data were used to produce efficient hydrological modelling outputs (Y. Zhang & Thorburn, 2022). A Double Mass Curve (DMC) technique was used to verify the consistency of the hydro-meteorological dataset (Sriwongsitanon et al., 2023). This method compares data from a single station with the cumulative average of all other stations in the area under consideration (Sriwongsitanon et al., 2023). Homogeneity tests were used to assess how changes in measurement instruments, observation methods, station locations, and nearby conditions affected climate data over time (Sriwongsitanon et al., 2023).

Table 1 | List of selected stations and details

Station		Latitude [°N]	Longititude [°E]	Altitude [m]	Missing Prec [%]
S.No	Name				
1	Arba Minch	6.06222	37.5614	1220	0.11%
2	Danna_2	6.58806	37.5508	1312	4.42%
3	Konso	5.34306	37.4383	1431	3%
4	Mirab Abaya Ber Ber	6.27361	37.7706	1221	1.57%
5	Alaba Kulito	7.31058	38.0939	1772	1.17%
6	Angacha	7.34528	37.8611	2321	8.24%
7	Hosana	7.56778	37.8561	2306	1.21%
8	Billate-Tena	6.82222	38.0878	1361	1.82%
9	Dilla	6.38056	38.3069	1515	3.93%
10	Wolaita	6.82167	37.7489	1854	0.03%
11	Awassa	7.065	38.4831	1694	0.05%

For this study, XLSTAT (2015.5.01) software was applied to evaluate the homogeneity test on a time series (https://www.xlstat.com). This statistical program was used to explore, visualize, and analyze complex multivariate data (Vidal et al., 2020). The XLSTAT software system integrates a comprehensive suite of functionalities, encompassing data preparation, machine learning–based exploration, and data visualization tools (https://www.xlstat.com).

An analysis of long-term daily precipitation records showed that the sub-basin received an average of 1,150 millimeters of precipitation per year. However, there was a significant variation in precipitation across space and time. For example, the highest and lowest recorded mean annual precipitation were 1,458 mm and 811 mm at the Angacha and Mirab-Abaya stations, respectively (see Figure 2). Mean annual precipitation was mapped across six main watersheds and two lakes. These watersheds included the Bilate River, Gidabo, Gelana, Sile, Amesa-Guracha, Kulfo-Hare, and Abaya-Chamo lakes. The highest annual precipitation occurred in the Gidabo Watershed, the northern part of the Amesa-Guracha Watershed, and the southwest part of the Bilate River Watershed. The lowest precipitation occured in the Sile, Kulfo-Hare, Gelana, and southern Bilate River Watersheds.

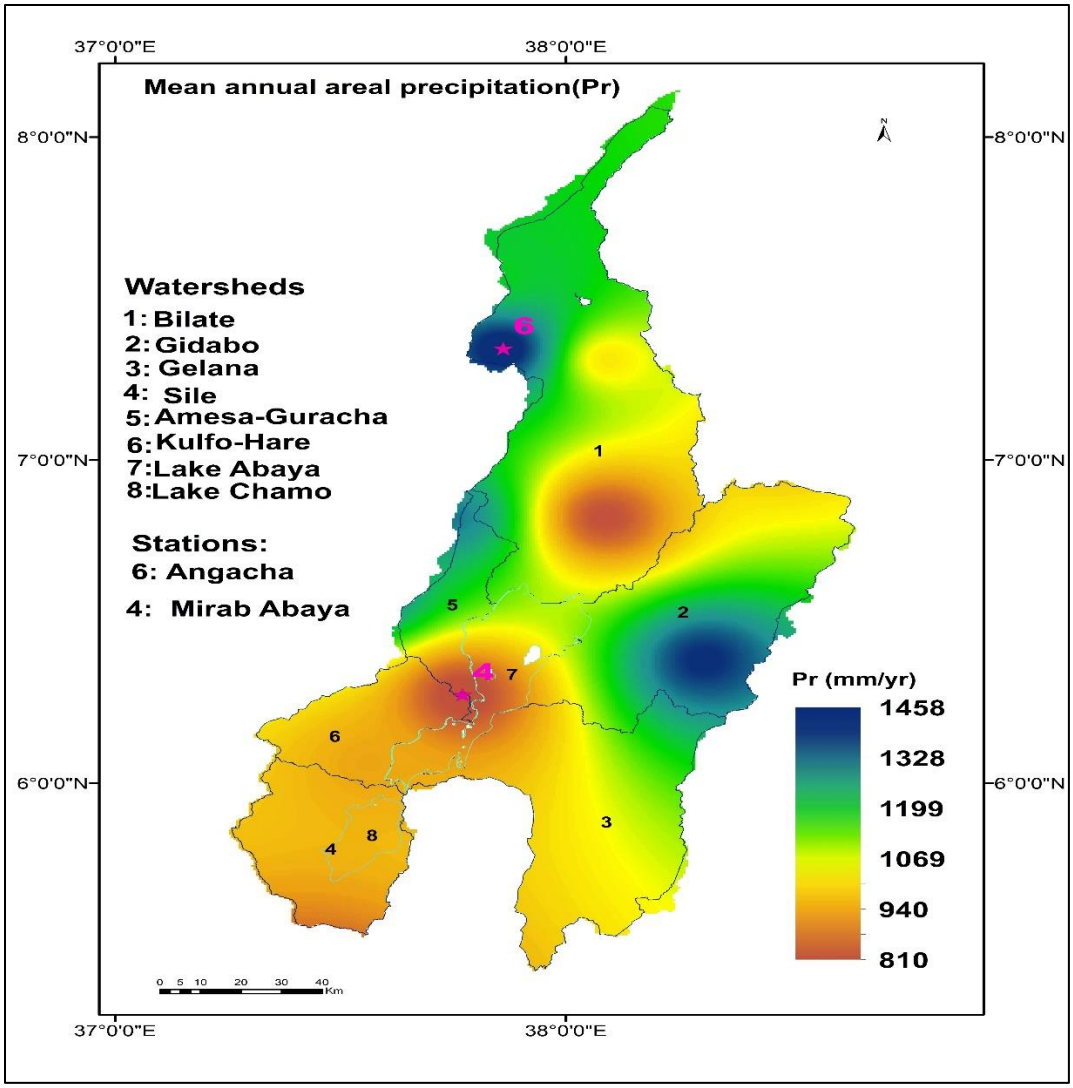

Figure 2 | Mean annual areal precipitation (mm/yr) distribution over the catchments (1992–2020) and two stations with the highest and lowest precipitation. The catchments are numbered with black numbers from 1 to 8, and the two extreme stations, namely Angacha and Mirab Abaya stations, are numbered 6 and 4 with purple color, respectively.

2.1.2 Global Climate Models

The Coupled Model Intercomparison Project Phase 6 model data are available on the Earth Systems Grid Federation portal (https://esgf-node.llnl.gov/search/cmip6, accessed on 20th August 2023). The outputs of general circulation models inherit uncertainties from various oversimplifications, assumptions, and parameterizations which affect the accuracy of climate simulations (Eyring et al., 2016). Therefore, employing multi-model ensembles instead of single-model approaches improved climate change projections by synthesizing outputs from

several models (Yimer et al., 2022; Zhu et al., 2023). This also helps to mitigate the inherent uncertainties of individual models.

In this study, the climate change impact scenarios were modeled using multi-model ensemble simulations under shared socio-economic pathways scenarios. The multi-model ensemble (MME) mean was calculated using six global climate models. The six GCMs with the best performances for replicating observations were chosen from a previous study that assessed 20 CMIP6 performance models over the study area (Ersado & Awoke, 2024). The chosen models were EC-Earth-CC, CNRM-CM6-1-HR, EC-Earth3, MPI-ESM1-2-HR, EC-Earth3-Veg-LR, ACCESS-CM2, and MPI-ESM1-2-HR. Their spatial resolutions ranged from 0.70^0 x 0.70^0 to 1.80^0 x 1.80^0 grids (Table 2). Table 2 lists the GCMs used, their institutions, and spatial resolutions. The study assessed climate change effects on sub-basin precipitation for the years 2021-2064 and 2065-2100 under SSP2-4.5 and SSP5-8.5 scenarios. Both SSP2-4.5 and SSP5-8.5 represented moderate energy pathways ^ with radiative forcing of about 2.6 W m^{-2}, and high energy pathways with radiative forcing of 8.5 W m^{-2}, respectively (Eyring et al., 2016).

Table 2 |List and detailed information of CMIP6 models

Model	**Institution**	**Original spatial Resolution(^{0})**
EC-Earth-CC	EC-EARTH consortium, Europe	0.70× 0.70
EC-Earth3	Consortium of European meteorological institutes and research centers, Europe	0.70× 0.70
ACCESS-CM2	Commonwealth science and industrial research organization(CSIRO), and the Australian Bureau of Meteorology	1.25 × 1.875
MPI-ESM1-2-LR	Max Planck Institute for Meteorology (MPI), Germany	1.88×1.88
CNRM-CM6-1-HR	Centre National de Recherches Météorologiques (CNRM) and CERFACS.	1.41 × 1.41
EC-Earth3-veg-LR	EC-EARTH consortium, Europe	1.125 x 1.125

2.2 Interpolation and Bias Correction

Climate model simulations commonly exhibit inherent systematic biases in their precipitation projections (Onyutha et al., 2021). Therefore, climate model outputs are typically inadequate for direct application in local climate change impact investigations (Onyutha et al., 2021). Hence, interpolation and bias correction are two essential techniques used to enhance the accuracy

of climate projections.

2.2.1 Spatial Interpolation Method

The chosen GCMs (Table 2) had spatial resolutionswhich were too coarse to use them for regional studies. Therefore, we couldnot use them directly to assess climate change effects on precipitation without interpolation and bias correction. Spatiotemporal interpolation was employed to deliver high-resolution climatic information for hydrometeorological modeling (Cerón et al., 2021). Thus, the coarse-resolution anomalous fields of the CMIP6 GCMs datasets were re-gridded to the observational reanalysis dataset' grid. The six GCM coarse resolution anomaly fields were regridded and interpolated to match the ERA5-Land dataset resolution.

The ERA5 reanalysis is the latest fifth-generation global climate reanalysis output developed by the European Center for Medium-Range Weather Forecasts' (ECMWF) latest fifth-generation global climate reanalysis (Hersbach et al., 2020). It was developed under the EU-funded Copernicus Climate Change Service (C3S) (https://climate.copernicus.eu). The ERA5 data sets were downloaded from the C3S Climate Data Store (https://cds.climate.copernicus.eu/accessed October 5, 2023) as 0.25° × 0.25° latitude–longitude grids.

Climate Data Operators (CDO) are command-line tools for statistical and arithmetic analysis of climate data (CDO, 2021). CDO handles climate data in NetCDF, SERVICE, EXTRA, IEG, and GRIB formats. There are more than 600 operators available for data informing, manipulating, formatting, and analyzing (CDO, 2021). In this study, we used Climate Data Operators (CDO) v2.0.5, developed by the Max Planck Institute, to interpolate and extract climate data. Daily precipitation of GCMs was interpolated using the bilinear interpolation method of CDO (CDO, 2021). CDO has no graphical user interface (GUI); commands can be run by installing Cygwin environment, Windows Subsystem for Linux (WSL), or Ubuntu's terminal running on Microsoft Windows (Sheldon, 2022). In this study, we used CDO with Cygwin terminal (https://www.cygwin.com/). Cygwin tools allowed UNIX or Linux application to compile and run on Windows through a Linux-like interface (Sheldon, 2022).

2.2.2 Model Bias-Correction Methods

Downscaled climate model output bias correction was used to enhance climate projections (Chandel et al., 2024). The bias correction technique applies a correction factor to adjust statistical measures of the output to better match the observed data (Chandel et al., 2024).

Globally, several studies employed different bias-correction methods techniques to correct bias of coarse-resolution general circulation models. This includes a linear scaling (Abdulahi et al., 2021); distribution mapping (Gurara et al., 2021); empirical quantile mapping (Voudouris, 2022); bias correction statistical downscaling (Rettie et al., 2023), and climate data bias-correcting (Gupta & Bhattarai, 2019). The statistical and dynamical downscaling methods were the most frequently used bias correction techniques (Rettie et al., 2023). Statistical downscaling methods produced downscaled climate data by forming empirical connections between broad-scale climate factors and local climatic conditions (Rettie et al., 2023). In addition, climatic model bias could be reduced using power transforming, distribution mapping, and empirical quantile mapping methods (Daniel, 2023; Tumsa, 2022; Worako et al., 2022). For instance, Tumsa (2022) used the power transforming and variance scaling methods for precipitation and temperature model data bias correction, respectively. Although Shrestha (2016) utilized power transformating to correct precipitation bias, it became an important method for reducing biases in simulated GCMs data based on the mean and variability of observation (Fang et al., 2015; Teutschbein & Seibert, 2012). In this study, the output of climate model s bias at each grid point was corrected by employing the power transformation (PT) method. The PT correction used the frequency-adjusted results from the local intensity scaling values (Luo et al., 2018; B. Zhang et al., 2018). The local intensity scaling method applied a wet-day threshold to adjust the mean, frequencies, and intensities of precipitation on wet days (B. Zhang et al., 2018) (Equation 2):

$$P^{1}_{con,m,d}=\begin{cases} P_{con,d}, \text{ if } P_{con,m,d} > P_{thres,m,d} \\ 0, \text{otherwise} \end{cases}$$

$$s_m=\frac{\mu(P_{obs,m,d}) \text{ if } \mu(P_{obs,m,d})>0}{\mu(P_{con,m,d}),\text{if } \mu(P_{obs,m,d})> P_{thres}} \qquad (2)$$

$$P^{Cor}_{con,m.d}=s_m \text{ x } P^{1}_{con,m,d}$$

Where, $P^{Cor}_{con,m.d}$ and $P^{1}_{con,m,d}$ are the corrected and transitional daily precipitation on the d^{th} day of the m^{th} month; $P_{con,m,d}$ and $P_{obs,m,d}$ are the original and observed precipitation on the corresponding d^{th} day of the m^{th} month, respectively, and s_m is the scaling factor.

The power transformation (PT) techniques apply an exponential nonlinear correction ($a P^b$) to adjust precipitation mean and variance (Teutschbein & Seibert, 2012) (Equation 3):

$$P^{Cor}_{hst,m.d}=s_{mu} \text{ x } P^{cor}_{con,m,d}$$

$$s_{mu}=\frac{\mu(P_{obs,m})}{\mu(P_{con,m.d}^{Cor})^{b_m}} \quad (3)$$

$$f(b_m)=\frac{\sigma(P_{obs,m})}{\mu(P_{obs,m})}-\frac{\sigma(P_{con,m.d}^{Cor})^{b_m}}{\mu(P_{con,m.d}^{Cor})^{b_m})}$$

where, $P_{hst,m.d}^{Cor}$ is the corrected precipitation for day (d) of the month (m); b_m is the month exponent, (σ) is the standard deviation, s_{mu} is the scaling factor, and (μ) is the mean value.

2.3 Characterization of the Mean Climatology

We used six downscaled, bias-corrected ensemble models to assess climate change impacts on future precipitation patterns. The corrected precipitation data were averaged daily, monthly, annually, and seasonally. The yearly precipitation value was calculated by summing up the daily precipitation rates for each day of the year. Seasonal precipitation values were calculated by summing up the daily rates in a specific season. The four seasons MAM, SON, DJF, and JJA were considered for the seasonal evaluation of precipitation change. Seasonal future precipitation patterns were computed for each season over the periods: 2021–2064 and 2065–2100. Historical long-term precipitation averages across the sub-basin were used for comparison. Projected precipitation change was the differences in GCM outputs for the baseline period (1992–2014) and future periods. Precipitation changes in monthly or annual amounts were calculated using Equation (4):

$$\Delta Pr,n,a=\frac{Pr_{fut,n,a}-Pr_{his,n,a}}{Pr_{his,n,a}} *100 \quad (4)$$

Where ΔPr, n, a is the annual precipitation change for month (n), $Pr_{fut,n,a}$ and $Pr_{his,n,a}$ are the future and historical annual precipitation values for that month.

Mean annual and seasonal precipitation spatial distribution maps for the Abaya-Chamo subbasin were created using inverse distance weighting (IDW) in ArcMap. These maps were used to identify areas of high and low rainfall distribution within each watershed.

3 RESULTS AND DISCUSSION

3.1 GCM Performance against Observations

The distribution of monthly mean observed precipitation exhibited a unimodal-to-bimodal rainfall regime with the majority of rainfall concentrated between March and September (Figure 3). A sharp increase was observed at the beginning of March, followed by the primary peak occurring between April and May. During April and May, stations like Dilla, Dana-2, Wolayita,

Angacha, and Arba Minch recorded average monthly rainfall above 150–220 mm. Following the early peak season, precipitation dropped sharply in June at several stations, including Konso and Arbaminch. However, some stations such as Angacha, Wolayita, and Dana-2 showed a second peak precipitation pattern in July–August, revealing spatial differences in rainfall patterns. In September, precipitation gradually declinedin all stations showing very little precipitation from October to January (Figure 3). During this time horizon, most stations recorded less than 50 mm of rain per month, defining a clear dry season. Overall, the precipitation distribution revealed intra-annual variability and noticeable spatial heterogeneity among the stations because of differences in topography, elevation, and local climatic factors.

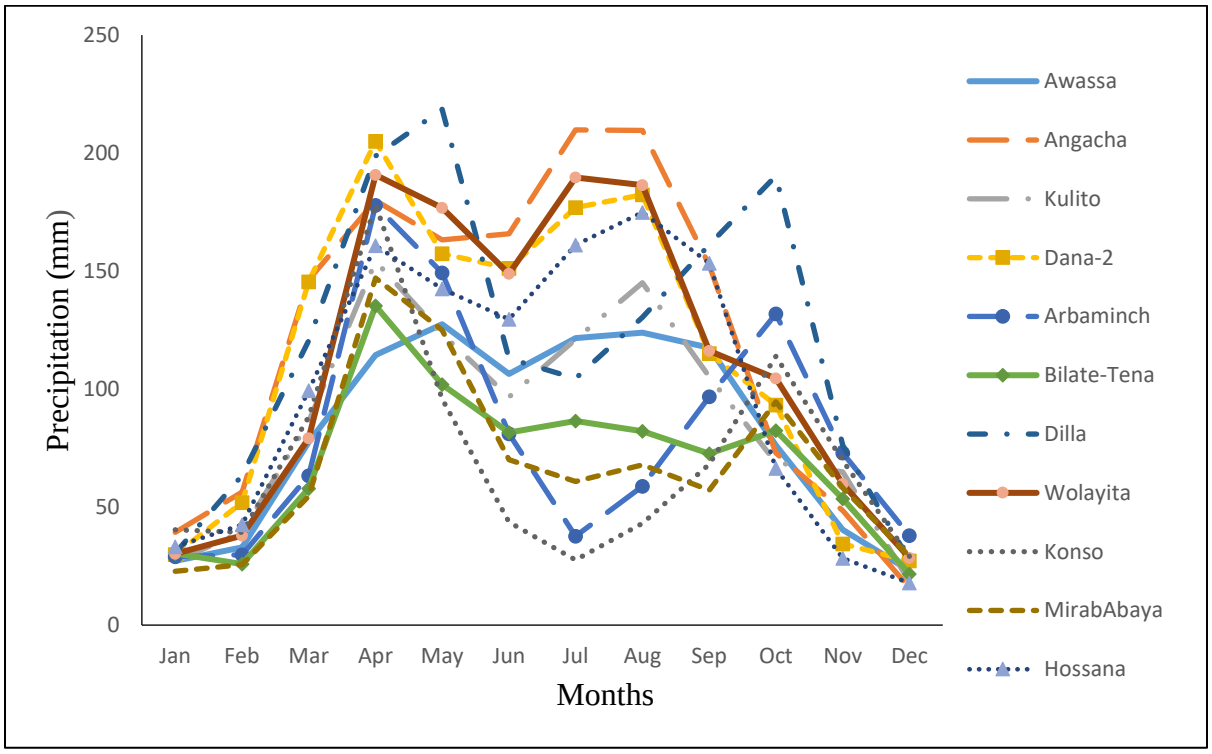

Figure 3 | Monthly mean observed precipitation distribution (1992-2020)

Multi-model ensemble biases were adjusted using observations from eleven gauge stations in and around the Abaya-Chamo sub-basin grid. First, we corrected the historical data for the baseline period (1992-2014). The performance of bias correction tool was evaluated by comparing the basin-level, multi-model monthly GCM averages with the mean observed value in the same period. This comparison confirmed the accuracy of the bias correction tool. As in Figure 4, the observed and bias-corrected data were compared graphically. The monthly average bias-

corrected GCM precipitation data series followed more closely the observed seasonal precipitation pattern over the base period. However, there were significant differences between the corrected multi-model ensemble (MME) outputs and the observations. The raw GCM ensemble simulations showed significant bias compared to observed precipitation data. From mid-March to August, the bias correction model underestimateed simulated precipitation whereas it overestimated from October to February. The bias-corrected data showed improved alignment with the raw climate model outputs from August to October owing to power transformation methods. which applied a power parameter. (Holthuijzen et al., 2022). Therefore, bias adjustment enhanced the match and introduced under-estimation for particularl extreme events when the original model bias was large or non-stationary (Holthuijzen et al., 2022; Padulano et al., 2025).

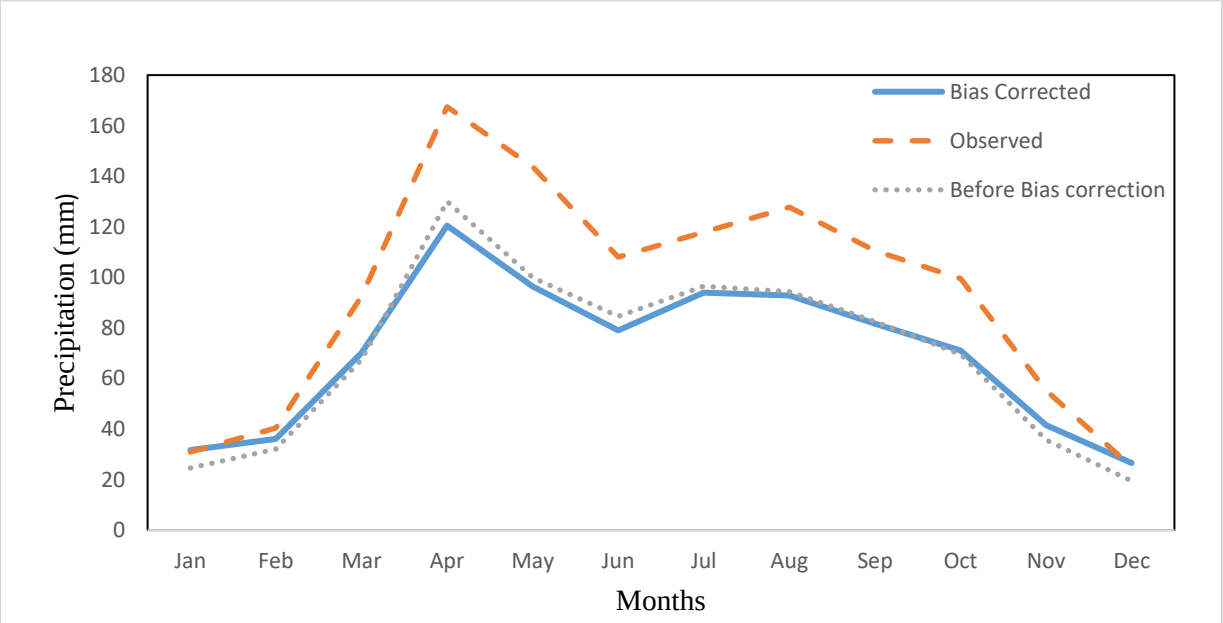

Figure 4 | Evaluation of the average observed precipitation data against multi-model GCM simulations during the baseline period, both prior to and following bias correction.

3.2 Spatial Pattern of Mean Seasonal Precipitation

Figure 5 shows the spatial distribution of observed and multi-model ensemble mean seasonal precipitation from 1992 to 2014. The seasonal patterns of observed and simulated GCM precipitation were grouped into winter, autumn, summer, and spring. The regionally averaged seasonal precipitation pattern showed that the corrected GCM multi-model ensemble

precipitation was similar to the observed precipitation particularly during the summer and autumn seasons.

During Autumn (SON), the corrected model ensemble mean (EM) typically exhibited higher values across all watersheds. The baseline precipitation simulation of climate model ensemble showed a relatively high degree of agreement with the measurements taken during the SON seasons in the eastern regions of the region. During this season, the southeastern part of the Gidabo Watershed experienced higher levels of precipitation.

During the JJA season, bias-corrected ensemble results showed closer agreement with the observed values in the northern and eastern regions, particularly in the Bilate and Amesa-Guracha watersheds. As shown in Figure 5, the northwestern portions particularly the Bilate River Watershed experienced high precipitation during the JJA season. In contrast, the southwestern portions, the Kulfo-Hare and Amesa-Guracha regions, experienced low precipitation. The area around the end of Lake Abaya and the confluences of most watersheds experienced minimal precipitation.

In the Bilate River Watershed, the bias-corrected ensemble simulation was lower than observed precipitation during the spring (MAM) season., . During the winter season (DJF), the corrected model ensemble mean (EM) typically exhibited lower values in all watersheds except in some parts of the Gidabo Watershed (Figure 5). The Intertropical Convergence Zone (ITCZ), El Niño and La Niña, topography variation, and atmospheric circulation patternswere the main factors causing seasonal precipitation variation in the Ethiopian Rift Valley Lakes Basin Niña (Ayalew et al., 2024).

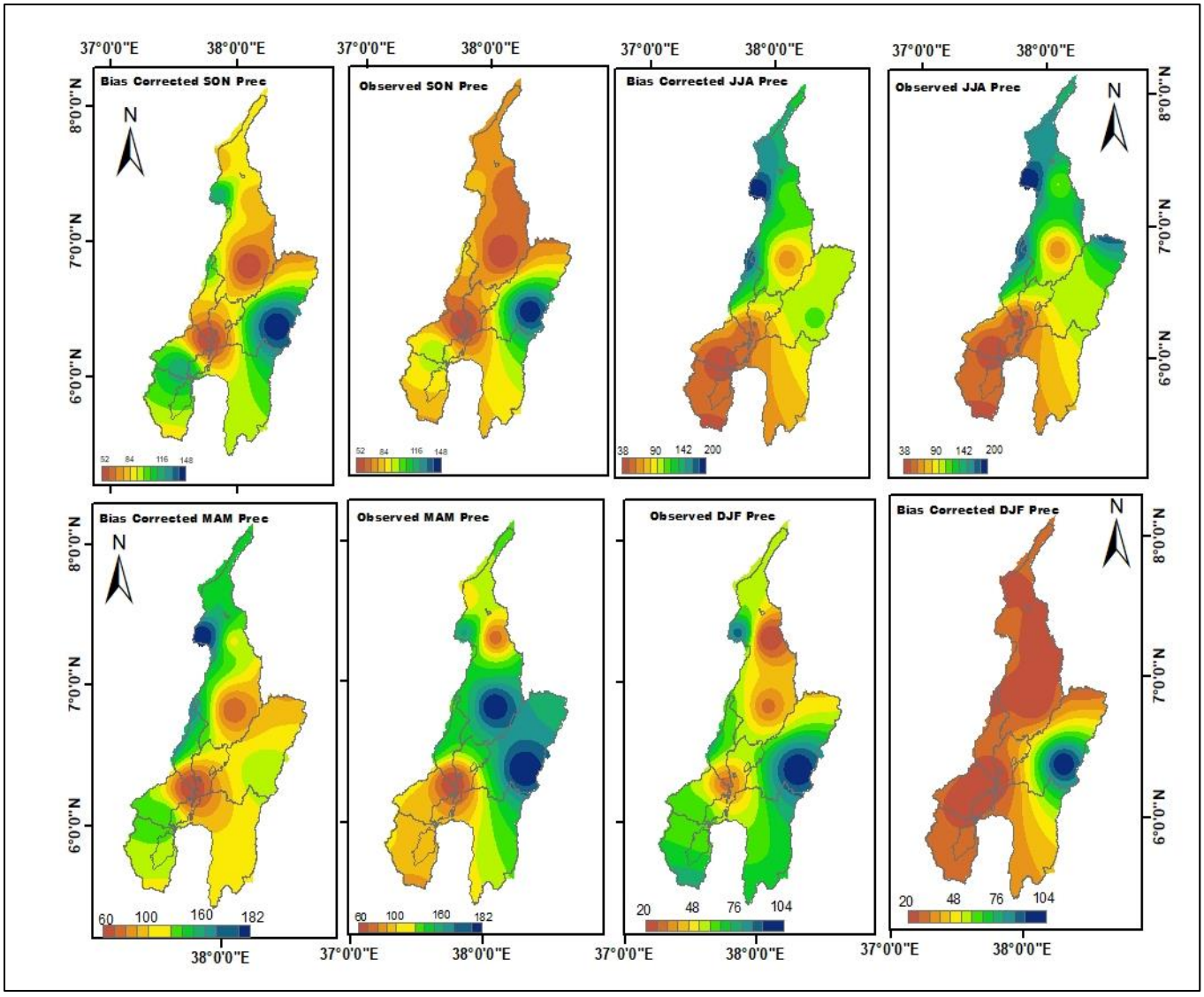

Figure 5 | Spatial pattern of mean observed and bias-corrected ensemble seasonal precipitation (mm/season) from 1992-2014 across the Abaya-Chamo sub-basin.

3.3 Climate Change Impact Analysis

3.3.1 Analysis of Future Precipitation

Future precipitation temporal analysis shows how precipitation patterns change over multiple time periods under various climate scenarios. Figure 6 presents predicted long-term monthly rainfall percentages in future scenarios. Results show a steady decline in average rainfall for 2021–2064 and 2065–2100 compared to historical levels.

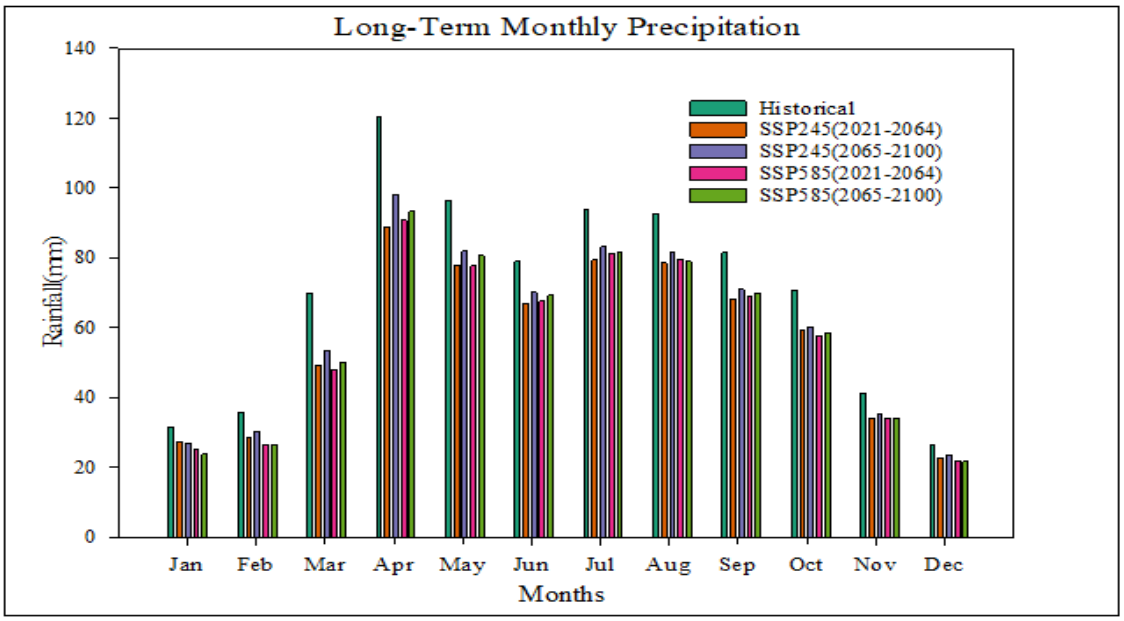

Figure 6 | A Comparative assessment of historical and future precipitation patterns

In the near-future period from 2021 to 2064, the anticipated changes in precipitation during both October to March and April to September are less significant under SSP2-4.5 compared to SSP5-8.5.However, in the far future period (2065-2100), projected precipitation under the SSP2-4.5 scenario is consistently lower across all months and regions compared to that under the SSP5-8.5 scenario The difference in the precipitation change between scenarios across different time periods primarily stemed from how each scenario altered atmospheric circulation, temperature, and moisture availability throughout the year (IPCC, 2021). In the distant future (2065-2100), changes in precipitation in both scenarios will be associated with increased temperature-driven moisture availability and extent of warming (Ayugi et al., 2021). During SSP5-8.5 scenarios, the larger warming, with regional temperature increase of 2 ˚c to 6°c was expected by the end of the century (Ayugi et al., 2021). Therefore, climate change under the SSP5-8.5 scenarios had a strong effect and led to a greater reduction in precipitation availability. In both scenarios, the projected decrease in precipitation will likely reduce water availability and groundwater levels in the future.

3.3.2 Mean Annual Precipitation Pattern

Figure 7 illustrates a bar graph depicting the anticipated changes in yearly precipitation for both the near and distant future under each scenario. The annual precipitation change results

corresponded to the difference between future modeled precipitation and the CMIP6 model ensemble from 1992 to 2014. Future seasonal and annual precipitation projections may indicate a decline in precipitation under the intermediate and high-emission scenarios. The intermediate and high-emission scenarios corresponded to the SSP2-4.5 and SSP5-8.5 scenarios, respectively (Eyring et al., 2016). The precipitation reduction magnitude varied by season, scenario, and time horizon (Asif et al., 2024). The strongest reductions were expected under the high-emission scenario during the late-century period. Annual precipitation showed a consistent decline across all scenarios ranging from approximately 18% to 22% under SSP2-4.5 and intensifying to 20% to 23% under SSP5-8.5. A previous study of the region revealed a potential decrease in mean annual precipitation ranging from 1.4% to 13.7% from 2016 to 2040 under RCP 8.5 scenarios (Gebeyehu, Chunju, Yihong, et al., 2019). Previous research by Hussen et al. (2018) suggested an increase and a decrease in rainfall under the RCP4.5 and RCP8.5 scenarios, respectively.

During the winter (DJF) season, precipitation was expected to decrease, ranging from around 18% in the SSP2-4.5 scenario (2021-2064) to nearly 28% in the SSP5-8.5 scenario at 2065-2100. In the near future, the precipitation pattern of the MAM season will decrease by up to 25% under the SSP2-4.5 scenario and by up to 27% under the SSP5-8.5 scenario.However, in the far future, the expected precipitation will decline under the scenarios SSP2-4.5 is 22% and SSP5-8.5 is 28 % (Figure 7). Generally, the greatest reduction in precipitation is anticipated during the winter months (DJF) under the SSP5-8.5 scenario and in the spring (MAM) for the SSP2-4.5 scenario. The maximum inter-annual decrease in seasonal precipitation variability highlights its vulnerability and climate change sensitivity (Belay et al., 2021). The pattern of precipitation during the spring season months was largely shaped by the early northward shift of the Intertropical Convergence Zone (ITCZ) and the transport of moisture from the Indian Ocean (Nicholson, 2017).

The seasonal assessment of the summer (JJA) indicated that precipitation reductions were less significant compared to those observed during the MAM and DJF seasons. The summer (JJA) precipitation changes were expected to decline from 14% to 18% during the SSP2.4.5 scenario. Similarly, medium to maximum reductions were expected to be observed during the SON season ranging from 12% to 17%. The findings indicated that projected changes in annual and seasonal precipitation were expected to reduce the water supply available to the ecosystems.

Consequently, it is essential to formulate effective water resource management strategies to adapt to these changes.

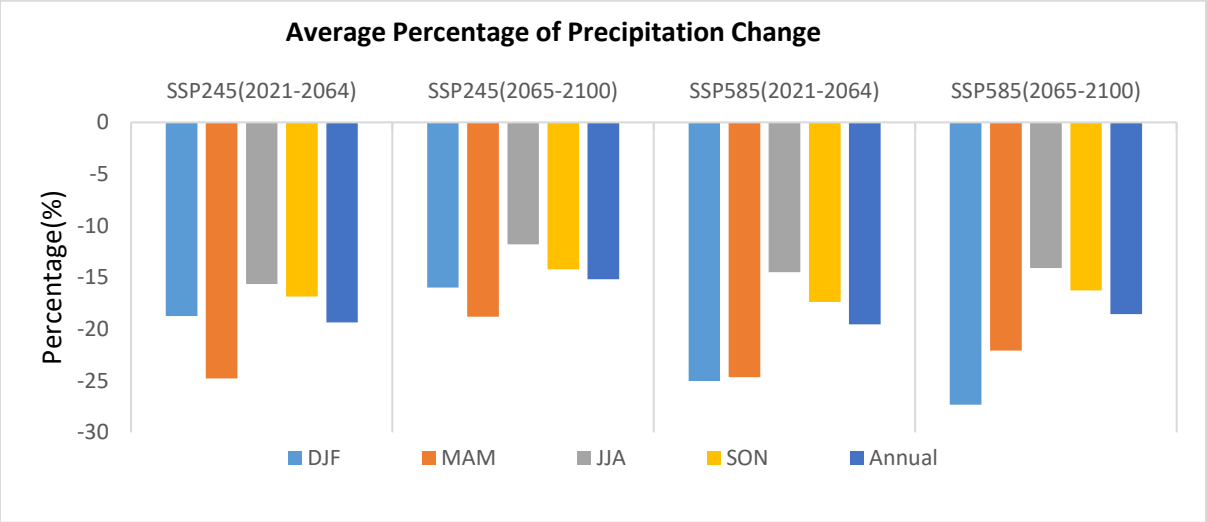

Figure 7 | Precipitation percentage changes for the near future and distant future periods

Figure 8 shows the projected shifts in the spatial distribution of average annual precipitation, based on the multi-model ensemble under SSP2-4.5 and SSP5-8.5 scenarios. For instance, under the SSP2-4.5 scenario from 2021 to 2064, annual precipitation ranged from 456.6 mm to 944.8 mm. Annual precipitation across the watersheds was projected to decrease by 6.6% to 25.9% in the near term (2021–2064) and by 5.3% to 20.2% in the long term (2065–2100). Under the SSP5-8.5 scenario, projected precipitation was estimated to be 465.8–936.8 mm for 2021–2064 and 454.3–939 mm for 2065–2100 (Figure 8). These ranges corresponded to precipitation changes of 7.4%-25.1% in the near future, and 7.2%-26.2% far future. In both SSP scenarios, the sub-basin projected mean annual precipitation change ranged from 5.2% to 26.5%. However, in the SSP2-4.5 and SSP5-8.5 scenarios, average annual precipitation in the sub-basin was projected to decrease by 15.2 % to 19.4 % and 18.5 % to 19.6 %, respectively (Figure 7). The average annual precipitation spatial distribution ranged from 450 to 1,140 mm across watersheds. For example, the eastern (Gidado watershed) and south-west (Bilate River watershed) regions of the basins received the most precipitation while the south-east (Sile watershed) and central parts (Abaya Chamo and the southern part of the Bilate River watershed) regions received the least precipitation. Under the SSP5-8.5 scenario, the Sile Watershed was anticipated to experience the greatest decline in average annual precipitation during the period 2065 to 2100. In contrast, the

Amesa-Guracha Basin was projected to experience the largest reduction during 2021–2064 under the SSP2-4.5 scenario. Annual mean precipitation in the Amesa-Guracha Watershed was projected to decline by 15.12%. In the Bilate River Watershed, annual average precipitation was expected to decrease by 18.6% under the SSP2-4.5 scenario for 2021–2064 and by 14.3% for 2065–2100. Likewise, under the SSP5-8.5, the Bilate River Watershed was projected to experience average annual precipitation reduction by 19.9% from 2021-2064 and 17.3 % from 2065-2100. This result conform with previous studies by Orke and Li (2022) who found that the annual average precipitation reduction in the Bilate River Watershed ranged from 6.5% to 38.3%. Similarly, Gebeyehu et al. (2019) reported that projected annual mean precipitation in the Bilate River Watershed decreased by 0.2% to 13.7%. under RCP scenarios for 2016-2040.

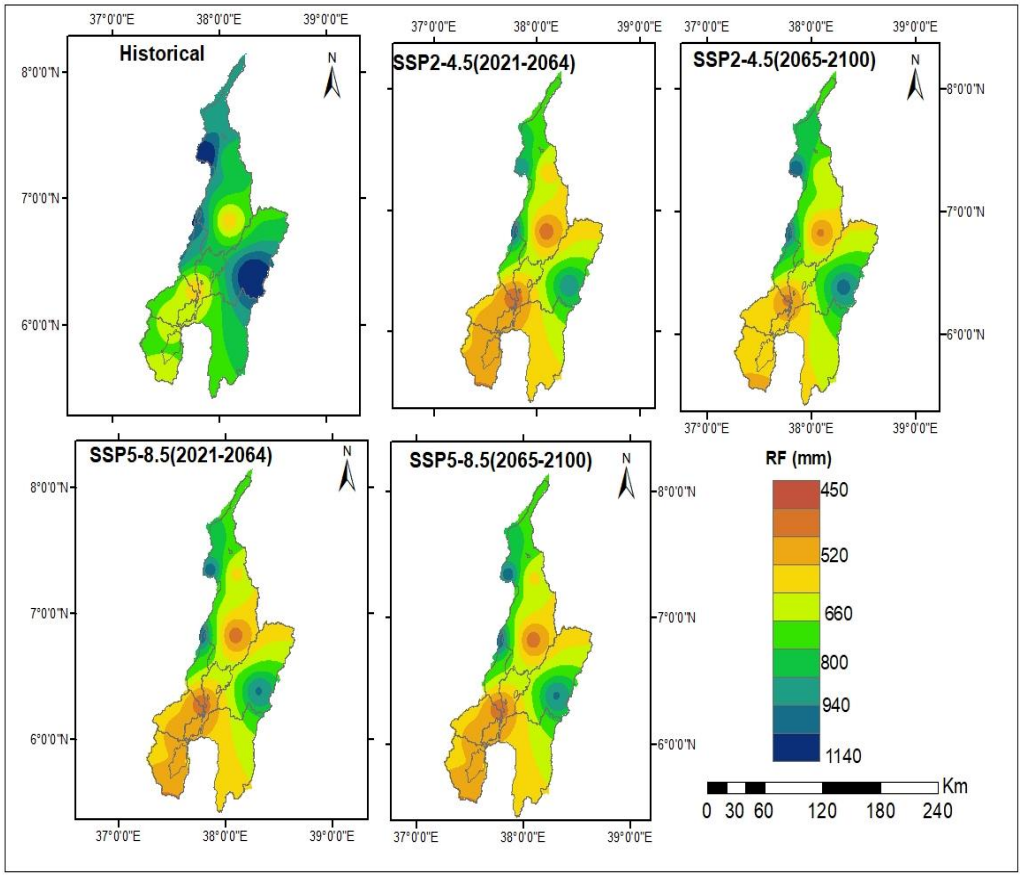

Figure 8 | Spatial patterns of annual mean precipitation (mm/year) across historical and future periods (2021–2064 and 2065–2100) under SSP2-4.5 and SSP5-8.5 scenarios

The projected annual mean precipitation in the south-east of the Gelana Watershed, decreased by up to 16.2% for the period from 2065 to 2100 under the SSP2-4.5 scenario. On the other hand,

under the SSP5-8.5 scenario, the mean annual precipitation was projected to be reduced up to 21.8 % during the period 2021-2064. This finding aligned with Daniel & Brook Abate (2022) who estimated a potential decrease of up to 15.12% in annual mean precipitation for the Gelana Watershed under the RCP4.5 scenario from 2051 to 2070. In the Gidabo Watershed, east part of the sub-basin, annual mean precipitation was projected to decline by 17.5 % during 2065-2100 under the SSP2-4.5 scenario and by 22.6 % for the period 2021-2064 under the SSP5-8.5 scenario. A research conducted by Alehu et al. (2022) on the Gidabo Watershed found that the annual mean precipitation was projected to reduce by 58.7 %, 34.5 %, and 62.2 % under RCP2.6, RCP4.5, and RCP8.5, respectively.

Therefore, the variability in projected precipitation change over the region suggested that some areas might be more affected than others. This highlighted the need for localized assessments and interventions. Overall, the multi-model ensemble from CMIP6 projects showed a decline in annual mean precipitation in the Abaya-Chamo Sub-basin in future periods. This finding was similar to previous studies (Chandel et al., 2024; Edamo et al., 2023; Orke & Li, 2022).

3.3.3 Seasonal Mean Distribution of Future Precipitation

Understanding seasonal climate patterns is crucial to effectively manage and sustain water resource availability (Konapala et al., 2020). Future climate pattern information enables stakeholders to make informed decisions, mitigate risks, and optimize resource use (Bizo et al., 2024). We performed a spatial analysis of seasonal mean precipitation with a multi-model ensemble for the historical period (1992–2014) and future period (2021–2100) under SSP2-4.5 and SSP5-8.5 scenarios, as shown in Figure 11 and 9. Seasonal precipitation changes corresponded to the difference between modeled future precipitation and the CMIP6 model ensemble for the corresponding season from 1992 to 2014. The seasonal mean precipitation change was anticipated to decline across the sub-basin under both scenarios (Table 3). However, the percentages of seasonal declines varied by season and watersheds in the sub-basin. For instance, during the 2021–2064 period, the seasonal mean precipitation in the autumn (SON) was projected to decline from 40 to 72 mm. This represented a decrease ranging from 0.33% to 26.41% compared to the historical ensemble simulation baseline (Table 3).

Table 3 |Seasonal future and historical precipitation change

Season	Percentages of Change (%)				
	Range	**SSP2-4.5 (2021-2064)**	**SSP2-4.5 (2065-2100)**	**SSP5-8.5 (2021-2064)**	**SSP5-8.5 (2065-2100)**
JJA	Min	0.40	-0.32	-0.40	-0.42
	Max	-27.12	-21.09	-26.42	-23.02
DJF	Min	-5.80	-4.19	-4.93	-8.72
	Max	-28.72	-26.88	-38.53	-42.58
MAM	Min	-13.02	-9.83	-13.84	-11.97
	Max	-44.90	-36.12	-34.81	-46.67
SON	Min	-0.33	-0.37	-0.45	-0.54
	Max	-24.14	-21.99	-26.41	-23.99

The Abay-Chamo Sub-basin had two major rainy seasons: spring and summer (Gebeyehu, Chunju, & Yihong, 2019). The predicted summer (JJA) seasonal mean precipitation droped slightly by 0.32 percent to 27.12 % and by 0.4 % to 26.42 % under the SSP2-4.5 and SSP5-8.5 scenarios, respectively. During JJA, the annual mean precipitation variability was expected to remain low across all scenarios. The maximum precipitation change during the JJA season ranged from 21.1% to 27.1%**.** The JJA season showed a significant reduction in peak precipitation under both scenarios. The summer season was an important rainy season for the basin; therefore, a decline in summer precipitation reduced the amount of runoff which could impact agriculture and water availability.

The seasonal mean precipitation reduction in the SON seasonwas between 0.33% to 24.14% in the SSP2-4.5 scenario, and 0.45% to 26.41% in the SSP5-8.5 scenario. During the SON season, the minimum precipitation change was between 0.33 % to 0.54 % while its maximum reductions ranged from 21.99 % and 26.41 %. A research by Edamo et al.(2023) indicated a similar trend to the current study, which showed a reduction in autumn seasonal (SON) precipitation ranging from 8.5% to 55.2%. The winter season (DJF) was naturally a dry season of the year (Kourouma et al., 2022); therefore, it exhibited substantial projected precipitation decline. The DJF season showed that minimum precipitation changes ranged from 4.19% to 8.72% while maximum reduction ranged from 26.88% to 42.58%. However, the largest decrease occurred under SSP5-8.5 in the late century. The Ethiopian Rift Valley Lake Basins were characterized by significant

climatic variability and experienced minimal precipitation during the winter season (Orke & Li, 2021)**.** During the MAM season, the projected mean precipitation from the multi-model ensemble decreased by 9.83% to 44.90% for the SSP2-4.5 scenario and by 11.97% to 46.67% for the SSP5-8.5 scenario. According to the SSP2-4.5 scenario, the mean precipitation during the MAM season was projected to decline by 13.02% to 44.90% between 2021 and 2064, and by 9.83% to 46.67% between 2065 and 2100. The mean precipitation during the MAM seasonwas expected to decrease by 13.84% to 34.81% and by 11.97% to 46.67% during the 2021-2064 and 2065-2100 periods respectively under the SSP5-8.5 high-reference scenario. MAM experienced the largest percentage reduction compared with all seasons. The MAM seasonwas expected to decline by 46% from 2065-2100 especially under the SSP5-8.5 scenario. The findings conformed to that of Edamo et al. (2023) who found a precipitation decline ranging from 1.45% to 53.8% using CMIP5 under RCP 4.5 and 8.5 in the Central Rift Valley (CRV) and Eastern Rift Valley (ERV). Overall, the SSP2-4.5 scenario showed a greater reduction tendency than the SSP5-8.5 scenario. These differencesarise from the varying socioeconomic, technological, and policy assumptions underlying each scenario (Eyring et al., 2018). The multi-model ensemble projections result revealed varying seasonal mean precipitation patterns across the sub-basin and within watersheds in future scenarios (Figure 10). For instance, the Gidabo Watershed was projected to undergo the greatest percentage of seasonal precipitation changes from 2065 to 2100 under the SSP2-4.5 scenario. Conversely, the Gelana Watershed was expected to experience the smallest change in precipitation during the same period under the SSP5-8.5 scenario. SON season future projections over the Bilate River Watershed indicated a decrease ranging from 14.13% to 18.1%. Edamo et al. (2022) and Lambe & Kundapura (2023) indicated that the Bilate River Watershed would experience significant precipitation variability particularly during the dry winter season. The average seasonal distribution of future precipitation patterns would be influenced by various interrelated factors such as climate change, geographical characteristics, and atmospheric dynamics (Paulos et al., 2022).

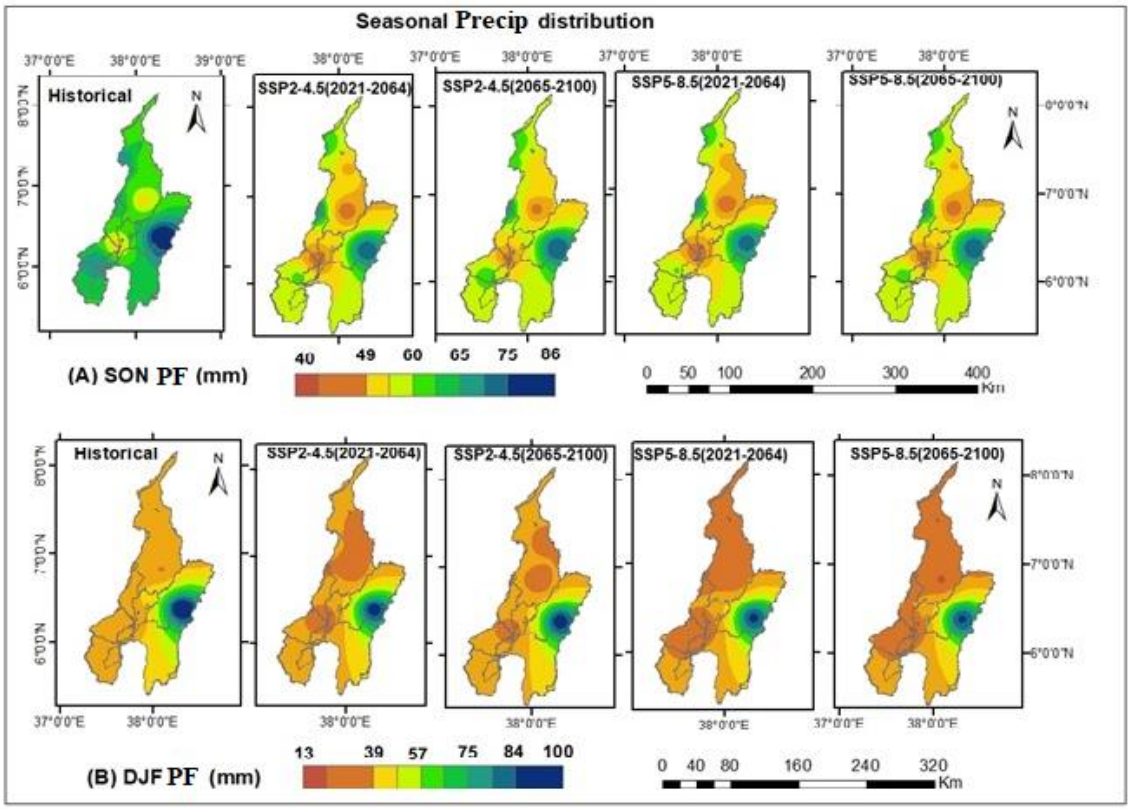

Figure 11 | Spatial patterns of seasonal mean precipitation (mm) for SON and DJF during the baseline and future periods.

The spatial variability of MAM precipitation compared to baseline precipitation could be minimal in the western sub-basin, i.e., north of the Amesa-Guracha Watershed and northwest of the Bilate River Watershed (

Figure **12**). It could be maximum in the eastern sub-basin, i.e., the Gidabo Watershed. The reduction in the projected MAM precipitation in the Bilate River Watershed ranged from 17.34% to 24.6%. However, Orke & Li (2022) demonstrated that summer (JJA) season precipitation experienced a maximum reduction of 51.5% and a minimum reduction of 11.2% with CanESM2-RCP8.5 and MPI-ESM-LR-RCP4.5, respectively.

In both scenarios, the JJA seasonal mean precipitation in the region was projected to reduce by 0.32% to 27.12%. The mean JJA precipitationwas expected to decrease significantly in the eastern region (the Gidabo Watershed) and to a lesser extent in the northwestern part (the Amasa-Guracha Watershed). The findings suggested that the JJA season multi-model ensemble precipitation projection showed greater reduction in the Gelana and Gidabo watersheds. Precipitation would decrease by 17.8% to 23% in the Gelana Watershed, whereas it would decrease by 18.7% to 24.4% in the Gidabo Watershed.

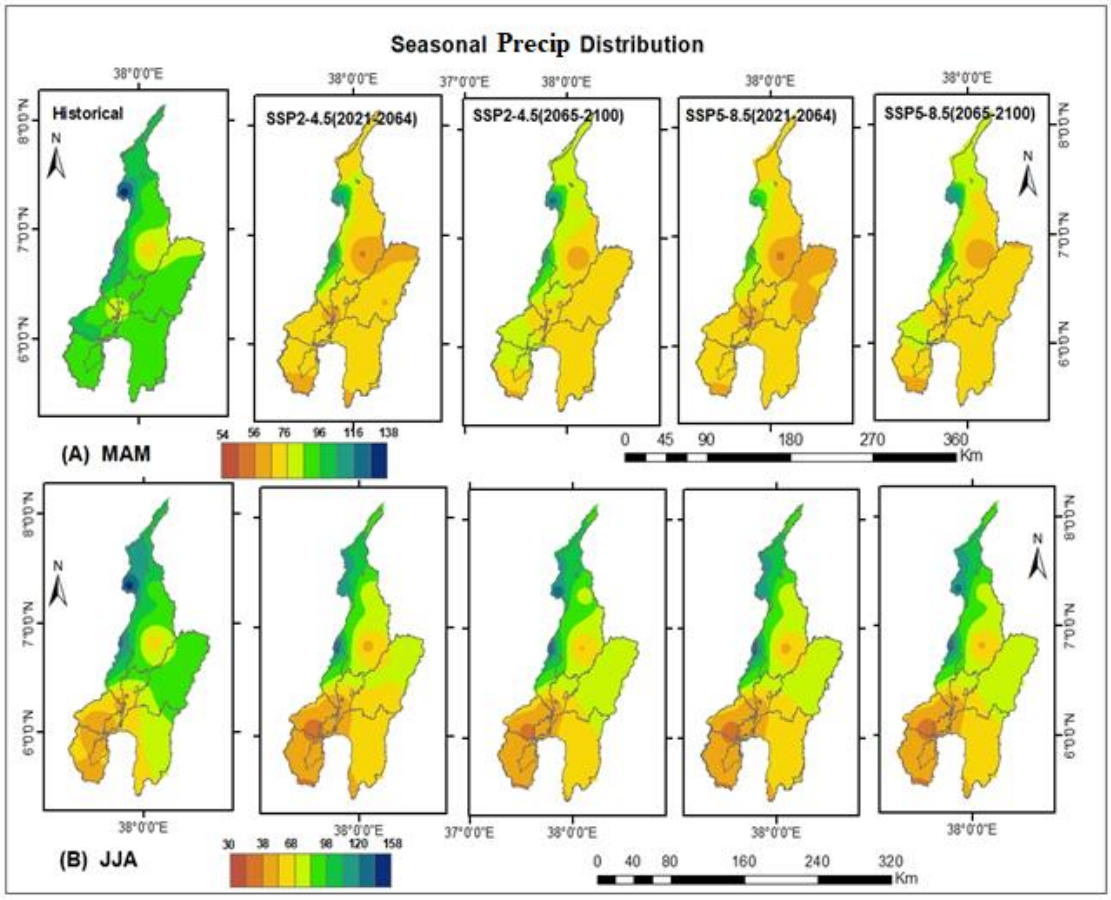

Figure 12 |Spatial distribution of the mean MAM and JJA season precipitation during the period of baseline and future periods.

4 CONCLUSION

This study evaluated how climate change affects future precipitation change in Abaya-Chamo Sub-basin under medium (SSP2-4.5) and high (SSP5-8.5) emissions scenarios. The six best multi-model ensemble (MME) outputs were selected for analysis of future precipitation change. The spatial patterns in the corrected multi-model ensemble precipitation output closely matched those observed in the historical period. The spatially interpolated and bias-corrected precipitation closely matched the observed precipitation data in the baseline period (1992-2014). Monthly mean precipitation projections showed a reduction during different periods under various scenarios. In both scenarios, annual average precipitation decreased by 15.7% to 25.5% and 11.8% to 27%, respectively. Seasonal precipitation projections under SSP2-4.5 and SSP5-8.5 indicated a consistent decline across all seasons in the region at near-future (2021–2064) and late-century (2065–2100) periods. The spatial distribution of the multi-model ensemble output

showed maximum mean precipitation in the Gidabo and Bilate River watersheds, and minimum mean precipitation in the Sile Watershed and the central region (Abaya and Chamo Lakes, and the southern part of the Bilate River Watershed). Seasonal precipitation projections under SSP2-4.5 scenarios indicated reductions ranging from 0.32% to 27.12% for JJA, 0.33% to 24.14% for SON, 9.83% to 44.9% for MAM, and 4.19% to 28.72% for DJF. Spring (MAM) and winter (DJF) were anticipated to experience the most pronounced reductions among the four seasons particularly under the high-emission SSP5-8.5 scenario. Meanwhile, the summer (JJA) and the autumn (SON) seasons exhibited moderate but consistent reductions particularly in their maximum precipitation values. The magnitude of the projected change in precipitation varied by season, scenario, and time horizon. In the high-emission SSP5-8.5 scenario, projected precipitation reductionswere greater than in the SSP2-4.5 scenario particularly in the late-century period. This difference was due to the distinct long-term socioeconomic, technological, and greenhouse gas emissions policies. The reduction in precipitation during different scenarios highlighted the susceptibility of the sub-basin to climate change. Overall, the results highlighted the urgent need for climate-adaptive water management strategies, improved monitoring, and local assessment.

Acknowledgments

The authors would like to thank the National Meteorological Agency (NMA) of Ethiopia for providing meteorological data. The authors would like to express their sincere gratitude to Addis Ababa University and Hawassa University for their guidance and support in conducting this research. The authors sincerely thank the anonymous reviewers for their constructive comments and valuable suggestions which significantly improved the quality and clarity of this manuscript.

Data Availability Statement

All relevant data and sources were included in the paper. The primary data would be accessed from the National Meteorological Agency upon request.

Funding: This research did not receive any specific external grants from funding Agencies.

Conflict of Interest: The authors declare that they have no known competing financial interests or personal relationships that would influence the study.

REFERENCES

Abdulahi, S. D., Abate, B., Harka, A. E., & Husen, S. B. (2021). *Uncorrected Proof Response of climate change impact on stream fl ow : the case of the Upper Awash Uncorrected Proof*. *00*(0), 1–22. https://doi.org/10.2166/wcc.2021.251

Al-husban, Y. (2022). Comparison of Spatial Interpolation Methods for Estimating the Annual Rainfall in the Wadi Al-Mujib Basin in Jordan. *Jordan Journal of Social Sciences*, *15*(2), 198–208. https://doi.org/10.35516/jjss.v15i2.490

Alehu, B. A., Desta, H. B., & Daba, B. I. (2022). Assessment of climate change impact on hydro-climatic variables and its trends over Gidabo Watershed. *Modeling Earth Systems and Environment*, *8*(3), 3769–3791. https://doi.org/10.1007/s40808-021-01327-w

Almazroui, M., Islam, M. N., Saeed, F., Saeed, S., & Ismail, M. (2021). Projected Changes in Temperature and Precipitation Over the United States , Central America , and the Caribbean in CMIP6 GCMs. *Earth Systems and Environment*, *5*(1), 1–24. https://doi.org/10.1007/s41748-021-00199-5

Almazroui, M., Saeed, F., Saeed, S., Islam, M. N., & Ismail, M. (2020). Projected Change in Temperature and Precipitation Over Africa from CMIP6. *Earth Systems and Environment*. https://doi.org/10.1007/s41748-020-00161-x

Alotaibi, K., Ghumman, A. R., Haider, H., Ghazaw, Y. M., & Shafiquzzama, M. (2018). Future Predictions of Rainfall and Temperature Using GCM and ANN for Arid Regions : A Case Study for. *Water*, *10*(1260). https://doi.org/10.3390/w10091260

Asif, M., Anjum, M. N., Azam, M., Hussain, F., Afzal, A., Kim, B. S., Maeng, S. J., Kim, D., & Iqbal, W. (2024). Climate-Driven Changes in the Projected Annual and Seasonal Precipitation over the Northern Highlands of Pakistan. *Water*, *16*(3461). https://doi.org/10.3390/w16233461

Ayalew, A. D., Wagner, P. D., Sahlu, D., & Fohrer, N. (2024). Unveiling hydrological dynamics in data-scarce regions: Experiences from the Ethiopian Rift Valley Lakes Basin. *Hydrology and Earth System Sciences*, *28*(8), 1853–1872. https://doi.org/10.5194/hess-28-1853-2024

Ayalew, A. T. (2023). The Synergic Effects of Climate Variability on Rainfall Distribution over Hare Catchment of Ethiopia. *Hindawi Advances in Meteorology*, *2023*(1175426), 20. https://doi.org/10.1155/2023/1175426

Ayenew, T., & Legesse, D. (2007). The changing face of the Ethiopian rift lakes and their environs : call of the time. *Lakes & Reservoirs: Research and Management 2007*, *12*, 149–165. https://doi.org/10.1111/j.1440-1770.2007.00332.x

Ayugi, B., Dike, V., Ngoma, H., Babaousmail, H., Mumo, R., & Ongoma, V. (2021). Future Changes in Precipitation Extremes over East Africa Based on CMIP6 Models. *Water*, *13*(2358), 1–20. https://doi.org/10.3390/w13172358

Ayugi, B., Shilenje, Z. W., & Babaousmail, H. (2022). Projected changes in meteorological drought over East Africa inferred from bias - adjusted CMIP6 models. *Natural Hazards*, *113*(2), 1151–1176. https://doi.org/10.1007/s11069-022-05341-8

Belay, A., Demissie, T., Recha, J. W., Oludhe, C., Osano, P. M., Olaka, L. A., Solomon, D., & Berhane, Z. (2021). Analysis of Climate Variability and Trends in Southern Ethiopia. *Climate*, *9*(96), 1–17. https://doi.org/10.3390/cli9060096

Bizo, I. M., Traore, B., & Soulé, M. (2024). Effectiveness of climate information services : an evaluation of the accuracy and socio-economic benefits for smallholder farmers in Niger and Mali. *Frontiers in Climate*, *6*(1345888). https://doi.org/10.3389/fclim.2024.1345888

Boke, A. S. (2017). Comparative Evaluation of Spatial Interpolation Methods for Estimation of

Missing Meteorological Variables over Ethiopia. *Journal of Water Resource and Protection*, *09*(08), 945–959. https://doi.org/10.4236/jwarp.2017.98063

CDO. (2021). Climate Data Operator(CDO) User Guide. In *MPI for Meteorology* (Issue October, pp. 1–237).

Cerón, W. L., Andreoli, R. V, Kayano, M. T., Canchala, T., Carvajal-escobar, Y., & Souza, R. A. F. (2021). Comparison of spatial interpolation methods for annual and seasonal rainfall in two hotspots of biodiversity in South America. *An Acad Bras Cienc*, *93*(1), 1–22. https://doi.org/10.1590/0001-3765202120190674

Chandel, V. S., Bhatia, U., Ganguly, A. R., & Ghosh, S. (2024). State-of-the-art bias correction of climate models misrepresent climate science and misinform adaptation . *Environ. Res. Lett.*, *19 (2024)*(094052), 1–47. https://doi.org/10.1088/1748-9326/ad6d82

Chang, S., Graham, W., Geurink, J., Wanakule, N., & Asefa, T. (2018). Evaluation of impacts of future climate change and water use scenarios on regional hydrology. *Hydrology and Earth System Sciences*, *22*(4793–4813), 4793–4813. https://doi.org/10.5194/hess-22-4793-2018

Chin, R. J., Lai, S. H., Loh, W. S., Ling, L., & Soo, E. Z. X. (2023). Assessment of Inverse Distance Weighting and Local Polynomial Interpolation for Annual Rainfall: A Case Study in Peninsular Malaysia †. *Engineering Proceedings*, *38*(1), 1–7. https://doi.org/10.3390/engproc2023038061

Daniel, H. (2023). Performance assessment of bias correction methods using observed and regional climate model data in different watersheds, Ethiopia. *Journal of Water and Climate Change*, *14*(6), 2007–2028. https://doi.org/10.2166/wcc.2023.115

Daniel, H., & Abate, B. (2022). Effect of climate change on streamflow in the Gelana watershed, Rift valley basin, Ethiopia. *Journal of Water and Climate Change*, *13*(5), 2205–2232. https://doi.org/10.2166/wcc.2022.059

Demmissie, N. G., Demissie, T. A., & Tufa, F. G. (2018). Predicting the Impact of Climate Change on Kulfo River Flow. *Hydrology*, *6*(3), 78–87. https://doi.org/10.11648/j.hyd.20180603.11

Deser, C., Phillips, A., & Bourdette, V. (2012). Uncertainty in climate change projections : the role of internal variability. *Clim Dyn*, *38*, 527–546. https://doi.org/10.1007/s00382-010-0977-x

Edamo, M. L., Bushira, K. M., Ukumo, T. Y., Ayele, M. A., Alaro, M. A., & Borko, H. B. (2022). Effect of climate change on water availability in Bilate catchment, Southern Ethiopia. *Water Cycle*, *3*(June), 86–99. https://doi.org/10.1016/j.watcyc.2022.06.001

Edamo, M. L., Hatiye, S. D., Minda, T. T., & Ukumo, T. Y. (2023). Flood inundation and risk mapping under climate change scenarios in the lower Bilate catchment, Ethiopia. *Natural Hazards*, *118*(3), 2199–2226. https://doi.org/10.1007/s11069-023-06101-y

Enawgaw, A., Asmare, A., Nigussie, B., Worku, D., & Fikru, A. (2023). Evaluating climate change impact on the hydrology of Kessie Watershed , Upper Blue Nile Basin , Ethiopia International Panel for Climate Change. *Applied Water Science*, *13*(7), 1–20. https://doi.org/10.1007/s13201-023-01947-w

Ersado, D. L., & Awoke, A. G. (2024). A multi-criteria decision analysis approach for ranking the performance of CMIP6 models in reproducing precipitation patterns over Abaya-Chamo sub-basin, Ethiopia. *Heliyon*, *10*(12). https://doi.org/10.1016/j.heliyon.2024.e32442

Eyring, V., Bony, S., Meehl, G. A., Senior, C. A., Stevens, B., Stouffer, R. J., Taylor, K. E., Dynamique, D. M., Pierre, I., Laplace, S., & Ipsl, L. M. D. (2016). *Overview of the Coupled Model Intercomparison Project Phase 6 (CMIP6) experimental design and organization*.

1937–1958. https://doi.org/10.5194/gmd-9-1937-2016

Eyring, V., Flato, G., Meehl, J., Senior, C., Stevens, B., Stouffer, R., Taylor, K., & Panel, C. (2018). *Overview of the Coupled Model Intercomparison Project Phase 6 (CMIP6) Experimental Design and Organization Coupled Model Intercomparison Project (CMIP). 6*. https://doi.org/10.5194/gmd-9-1937-2016

Fang, G. H., Yang, J., Chen, Y. N., & Zammit, C. (2015). *Comparing bias correction methods in downscaling meteorological variables for a hydrologic impact study in an arid area in China*. 2547–2559. https://doi.org/10.5194/hess-19-2547-2015

Gebeyehu, A. E., Chunju, Z., & Yihong, Z. (2019). Assessment and mapping of land use change by remote sensing and GIS: A Case Study of Abaya Chamo Sub-basin, Ethiopia. *Nature Environment and Pollution Technology*, *18*(2), 549–554.

Gebeyehu, A. E., Chunju, Z., Yihong, Z., & Wagasho, N. (2019). Drought event analysis and projection of future precipitation scenario in Abaya Chamo sub-basin, Ethiopia. *Journal of Engineering and Technological Sciences*, *51*(5), 707–728. https://doi.org/10.5614/j.eng.technol.sci.2019.51.5.8

Gupta, R., & Bhattarai, R. (2019). Development of Climate Data Bias Corrector (CDBC) Tool and Its Application over the Agro-Ecological. *Water*, *11*(1102). https://doi.org/10.3390/w11051102

Gurara, M. A., Jilo, N. B., & Tolche, A. D. (2021). Modelling climate change impact on the streamflow in the Upper Wabe Bridge watershed in Wabe Shebele River Basin, Ethiopia. *International Journal of River Basin Management*, *21*(2), 181–193. https://doi.org/10.1080/15715124.2021.1935978

Hersbach, H., Bell, B., Berrisford, P., Hirahara, S., Horányi, A., Nicolas, J., Peubey, C., Radu, R., Bonavita, M., Dee, D., Dragani, R., Flemming, J., Forbes, R., Geer, A., Hogan, R. J., Janisková, H. M., Keeley, S., Laloyaux, P., Cristina, P. L., & Thépaut, J. (2020). The ERA5 global reanalysis. *Quarterly Journal Ofthe Royal Meteorological Society*, *September 2019*, 1999–2049. https://doi.org/10.1002/qj.3803

Hırca, T., & Eryılmaz Türkkan, G. (2024). Assessment of Different Methods for Estimation of Missing Rainfall Data. *Water Resources Management*. https://doi.org/10.1007/s11269-024-03936-3

Holthuijzen, M., Beckage, B., Clemins, P. J., Higdon, D., & Winter, J. M. (2022). Robust bias-correction of precipitation extremes using a novel hybrid empirical quantile-mapping method Advantages of a linear correction for extremes. *Theoretical and Applied Climatology (2022)*, *149*(863), 863–882. https://doi.org/10.1007/s00704-022-04035-2

Hussen, B., Mekonnen, A., & Murlidhar, S. (2018). Integrated water resources management under climate change scenarios in the sub-basin of Abaya-Chamo , Ethiopia. *Modeling Earth Systems and Environment*, *0*(0), 0. https://doi.org/10.1007/s40808-018-0438-9

Hussen, B., & Wagesho, N. (2016). Regional Flood Frequency Analysis for Abaya – Chamo Sub-Basin, Rift Valley Basin Ethiopia. *Journal of Resources Development and Management*, *24*(January), 15–28.

IPCC. (2021). *Climate Change 2021 The Physical Science Basis Summary for Policymakers*.

IPCC. (2022). Summary for Policymakers. In *: Climate Change 2022: Impacts, Adaptation and Vulnerability. Contribution of Working Group II to the Sixth Assessment Report of the Intergovernmental Panel on Climate Change* (pp. 3–33). https://doi.org/10.1017/9781009325844.001

Jamal, K., Li, X., Chen, Y., Rizwan, M., Adnan, M., Syed, Z., & Mahmood, P. (2023). *Bias*

correction and projection of temperature over the altitudes of the Upper Indus Basin under CMIP6 climate scenarios from 1985 to 2100. *14*(7), 2490–2514. https://doi.org/10.2166/wcc.2023.180

Konapala, G., Mishra, A. K., Wada, Y., & Mann, M. E. (2020). precipitation and evaporation. *Nature Communications*, *11*(3044), 1–10. https://doi.org/10.1038/s41467-020-16757-w

Kourouma, J. M., Eze, E., Kelem, G., Negash, E., Phiri, D., Vinya, R., Girma, A., & Zenebe, A. (2022). Spatiotemporal climate variability and meteorological drought characterization in Ethiopia Spatiotemporal climate variability and meteorological. *Geomatics, Natural Hazards and Risk*, *13*(1), 2049–2085. https://doi.org/10.1080/19475705.2022.2106159

Lambe, B. T., & Kundapura, S. (2023). Recent Changes in Hydrometeorological Extremes in the Bilate River Basin of Rift Valley, Ethiopia. *Journal of Hydrologic Engineering*, *28*(7). https://doi.org/10.1061/jhyeff.heeng-5853

Luo, M., Liu, T., & Meng, F. (2018). *Comparing Bias Correction Methods Used in Downscaling Precipitation and Temperature from Regional Climate Models : A Case Study from the Kaidu River Basin in Western China*. https://doi.org/10.3390/w10081046

Mahyun, A. W., Mohd Azrul Ismail, M., Salwa, M. Z. M., Isa, N., Azlinda, A. G., & Fauzi, M. R. (2024). Comparison of the missing rainfall data method in enhancing discharge estimation. *IOP Conference Series: Earth and Environmental Science*, *1369*(1). https://doi.org/10.1088/1755-1315/1369/1/012045

Molla, D. D., Ayenew, T., & Fletcher, C. G. (2019). Simulated surface and shallow groundwater resources in the Abaya-Chamo Lake basin , Ethiopia using a spatially-distributed water balance model Journal of Hydrology : Regional Studies Simulated surface and shallow groundwater resources in the Abaya-Chamo L. *Journal of Hydrology: Regional Studies*, *24*(July), 100615. https://doi.org/10.1016/j.ejrh.2019.100615

Nicholson, S. E. (2017). Climate and climatic variability of rainfall over eastern Africa. *Reviews of Geophysics*, *55*, 590–635. https://doi.org/10.1002/2016RG000544

Omay, P. O., Muthama, N. J., Oludhe, C., Kinama, J. M., Artan, G., & Atheru, Z. (2023). Evaluation of CMIP6 historical simulations over IGAD region of Eastern Africa. *Discover Environment*. https://doi.org/10.1007/s44274-023-00012-2

Onyutha, C., Asiimwe, A., Ayugi, B., Ngoma, H., Ongoma, V., & Tabari, H. (2021). Observed and Future Precipitation and Evapotranspiration in Water Management Zones of Uganda : CMIP6 Projections. *Atmosphere*, *12*(887), 1–25. https://doi.org/10.3390/atmos12070887

Orke, Y. A., & Li, M. (2021). Hydroclimatic Variability in the Bilate Watershed, Ethiopia. *Climate*, *9*(98). https://doi.org/doi.org/10.3390/ cli9060098

Orke, Y. A., & Li, M. H. (2022). Impact of Climate Change on Hydrometeorology and Droughts in the Bilate Watershed, Ethiopia. *Water (Switzerland)*, *14*(5). https://doi.org/10.3390/w14050729

Padulano, R., Gomez-mogollon, L. A., Napolitano, L., & Rianna, G. (2025). Quantile-based bias-correction of extreme rainfall : Pros & cons of popular methods for climate signal preservation. *Journal of Hydrology*, *653*(August 2024), 132814. https://doi.org/10.1016/j.jhydrol.2025.132814

Paulos, T., Kranjac-berisavijevic, G., & Abagale, F. K. (2022). Impact of climate change on future precipitation amounts , seasonal distribution , and stream flow in the Omo-Gibe basin , Ethiopia. *Heliyon*, *8*(6). https://doi.org/10.1016/j.heliyon.2022.e09711

Rastogi, D., Kao, S., & Ashfaq, M. (2022). *How May the Choice of Downscaling Techniques and Meteorological Reference Observations Affect Future Hydroclimate Projections ?*

Earth ' s Future. https://doi.org/10.1029/2022EF002734

Rettie, F. M., Gayler, S., Weber, T. K. D., Tesfaye, K., & Streck, T. (2023). High-resolution CMIP6 climate projections for Ethiopia using the gridded statistical downscaling method. *Scientific Data*, *10*(442), 1–18. https://doi.org/10.1038/s41597-023-02337-2

Sheldon, R. (2022). *What is Cygwin and how does it work?* (p. 1). https://www.techtarget.com/searchdatacenter/definition/Cygwin%0A.

Shrestha, M. (2016). *Data analysis relied on Power Transformation of rainfall bias correction (V.2.0) Microsoft Excel tool. https://doi.org/10.13140/RG.2.1.5025.3200*.

Sriwongsitanon, N., Kaprom, C., Tantisuvanichkul, K., & Prasertthonggorn, N. (2023). The Combined Power of Double Mass Curves and Bias Correction for the Maximisation of the Accuracy of an Ensemble Satellite-Based Precipitation Estimate Product. *Hydrology*, *10*(154). https://doi.org/10.3390/hydrology10070154

Stawowy, M., Olchowik, W., Rosinsiki, A., & ˛abrowski, T. D. (2021). The Analysis and Modelling of the Quality of Information Acquired from Weather Station Sensors. *Remote Sens.*, *13*(693), 1–18.

Suksatit, P., Thongudom, B., & Khunthong, C. (2025). Assessment of Carbon Footprint from Integrated Innovation Camp Activities. *EnvironmentAsia*, *18*(Special), 133–142. https://doi.org/10.14456/ea.2025.29

Temesgen, E. E., ARERU, D. A., Arba, & WENDEMENEH, D. (2022). THE IMPACT OF CLIMATE CHANGE ON THE RIFT-VALLEY LAKES BASIN IN SOUTHERN ETHIOPIA : A REVIEW. ETHIOPIA. *Journal of Digital Food, Energy & Water Systems*, *3*(1), 1–15.

Teutschbein, C., & Seibert, J. (2012). Bias correction of regional climate model simulations for hydrological climate-change impact studies : Review and evaluation of different methods. *Journal of Hydrology*, *456–457*, 12–29. https://doi.org/10.1016/j.jhydrol.2012.05.052

Tumsa, B. C. (2022). Performance assessment of six bias correction methods using observed and RCM data at upper Awash basin , Oromia , Ethiopia. *Journal of Water and Climate Change*, *13*(2), 664–683. https://doi.org/10.2166/wcc.2021.181

Umugwaneza, A., Chen, X., Liu, T., Li, Z., Uwamahoro, S., Mind, R., Umwali, E. D., Ingabire, R., & Uwineza, A. (2021). Future Climate Change Impact on the Nyabugogo Catchment Water Balance in Rwanda. *Water 2021, 13*(3636), 1–18. https://doi.org/10.3390/w13243636

Vidal, N. P., Manful, C. F., Pham, T. H., Stewart, P., Keough, D., & Thomas, R. (2020). MethodsX The use of XLSTAT in conducting principal component analysis (PCA) when evaluating the relationships between sensory and quality attributes in grilled foods. *MethodsX*, *7*, 100835. https://doi.org/10.1016/j.mex.2020.100835

Voudouris, K. (2022). Spatio-Temporal Interpolation and Bias Correction Ordering Analysis for Hydrological Simulations : An Assessment on a Mountainous River Basin. *Water*, *14*(660). https://doi.org/10.3390/w14040660

Wen, K., Gao, B., & Li, M. (2021). Quantifying the Impact of Future Climate Change on Runoff in the Amur River Basin Using a Distributed Hydrological Model and CMIP6 GCM Projections. *Atmosphere*, *12*(1560). https://doi.org/10.3390/atmos12121560

WMO. (2011). *Guide to Climatological Practices 2011* (Issue 100).

Worako, A. W., Haile, A. T., & Taye, M. T. (2022). Implication of bias correction on climate change impact projection of surface water resources in the Gidabo sub-basin, Southern Ethiopia. *Journal of Water and Climate Change*, *13*(5), 2070–2088. https://doi.org/10.2166/wcc.2022.396

Yimer, S. M., Bouanani, A., Kumar, N., Tischbein, B., & Borgemeister, C. (2022). Assessment of Climate Models Performance and Associated Uncertainties in Rainfall Projection from CORDEX over the Eastern Nile Basin, Ethiopia. *Climate*, *10*(7). https://doi.org/10.3390/cli10070095

Zhang, B., Shrestha, N. K., Daggupati, P., Rudra, R., & Shukla, R. (2018). *Quantifying the Impacts of Climate Change on Streamflow Dynamics of Two Major Rivers of the Northern Lake Erie Basin in Canada*. https://doi.org/10.3390/su10082897

Zhang, Y., & Thorburn, P. J. (2022). Handling missing data in near real-time environmental monitoring : A system and a review of selected methods. *Future Generation Computer Systems*, *128*, 63–72. https://doi.org/10.1016/j.future.2021.09.033

Zhu, H., Jiang, Z., Li, L., Li, W., Jiang, S., Zhou, P., Zhu, H., Jiang, Z., Li, L., Li, W., & Jiang, S. (2023). Intercomparison of multi-model ensemble-processing strategies within a consistent framework for climate projection in China To cite this version : HAL Id : hal-04293706. *Science China Earth Sciences*, *66*(9), pp2125-2141. https://doi.org/10.1007/s11430-022-1154-7 .